Common Channels for Water and Protons at Apical and Basolateral Cell Membranes of Frog Skin and Urinary Bladder Epithelia

Effects of Oxytocin, Heavy Metals, and Inhibitors of H^+-Adenosine Triphosphatase

BRIAN HARVEY, ISABELLE LACOSTE, and JORDI EHRENFELD

From the Laboratoire Jean Maetz, Département de Biologie, Commissariat à l'Energie Atomique, F-06230 Villefranche-sur-mer, France

ABSTRACT   We have compared the response of proton and water transport to oxytocin treatment in isolated frog skin and urinary bladder epithelia to provide further insights into the nature of water flow and H^+ flux across individual apical and basolateral cell membrances. In isolated spontaneous sodium-transporting frog skin epithelia, lowering the pH of the apical solution from 7.4 to 6.4, 5.5, or 4.5 produced a fall in pH_i in principal cells which was completely blocked by amiloride (50 μM), indicating that apical Na^+ channels are permeable to protons. When sodium transport was blocked by amiloride, the H^+ permeability of the apical membranes of principal cells was negligible but increased dramatically after treatment with antidiuretic hormone (ADH). In the latter condition, lowering the pH of the apical solution caused a voltage-dependent intracellular acidification, accompanied by membrane depolarization, and an increase in membrane conductance and transepithelial current. These effects were inhibited by adding Hg^{2+} (100 μM) or dicyclohexylcarbodiimide (DCCD, 10^{-5} M) to the apical bath. Net titratable H^+ flux across frog skin was increased from 30 ± 8 to 115 ± 18 neq·h^{-1}·cm^{-2} ($n = 8$) after oxytocin treatment (at apical pH 5.5 and serosal pH 7.4) and was completely inhibited by DCCD (10^{-5} M). The basolateral membranes of the principal cells in frog skin epithelium were found to be spontaneously permeable to H^+ and passive electrogenic H^+ transport across this membrane was not affected by oxytocin. Lowering the pH of the basolateral bathing solution (pH_b) produced an intracellular acidification and membrane depolarization (and an increase in conductance when the normal dominant K^+ conductance of this membrane was abolished by Ba^{2+} 1 mM). These effects of low pH_b were blocked by micromolar concentrations of heavy metals (Zn^{2+}, Ni^{2+}, Co^{2+}, Cd^{2+}, and Hg^{2+}). Lowering pH_b in the presence of oxytocin

Address reprint requests to Dr. Brian J. Harvey, Laboratoire Jean Maetz, Département de Biologie, Commissariat à l'Energie Atomique, Station Marine B.P. 68, F-06230 Villefranche-sur-mer, France.

(50 mU/ml) produced a transepithelial current (3 $\mu A \cdot cm^{-2}$ at pH_b 5.5) which was blocked by 100 μM of Hg^{2+}, Zn^{2+}, or Ni^{2+} at the basolateral side, and by DCCD (10^{-5} M) or Hg^{2+} (100 μM) from the apical side. The net hydroosmotic water flux (J_{H_2O}) induced by oxytocin in frog bladder sacs was blocked by inhibitors of H^+-adenosine triphosphatase (ATPase). Diethylstilbestrol (DES 10^{-5} M), oligomycin (10^{-8} M), and DCCD (10^{-5} M) prevented J_{H_2O} when present in the lumen. These effects cannot be attributed to inhibition of metabolism since cyanide (10^{-4} M), or 2-deoxyglucose (10^{-3} M) had no effect on J_{H_2O}. DCCD and oligomycin, which are known to interact with the F_o proton channel of F_1-F_o H^+-ATPase also appear to act directly on the apical water channel in glutaraldehyde-fixed bladders. The sulfhydryl group reagent n-ethylmaleimide (10^{-4} M) which interacts with the F_1-F_o-type H^+-ATPase in renal epithelia as well as vacuolar H^+-ATPase produced an 85% inibition of J_{H_2O}. Oxytocin failed to activate a net water flux when Zn^{2+} (100 μM) or Hg^{2+} (100 μM) were present in the serosal solution, or if Hg^{2+} (but not Zn^{2+}) was added to the lumen. J_{H_2O} was sensitive to transitional heavy metals in the same concentration range which produced block of basolateral membrane H^+ conductance. Net water flux and titratable H^+ flux (J_{H^+}) measured simultaneously in frog bladder showed similar time dependence in their activation and inactivation responses to oxytocin. Both J_{H_2O} and J_{H^+} were equally inhibited by serosal Zn^{2+} (100 μM) or DES (10^{-5} M) and by luminal DCCD (10^{-5} M). We conclude that the basolateral cell membranes of frog skin and urinary bladder epithelia possess spontaneously open channels permeable to water and protons which can be blocked by micromolar cencentrations of heavy metals. In the presence of oxytocin and favorable concentration gradients, J_{H_2O} and rheogenic H^+ permeation can share a common pathway (F_o-type channel?) at the apical membrane. These similarities between water and proton transport may be exploited in the characterization of "water channels" at apical and basolateral cell membranes.

INTRODUCTION

Antidiuretic hormone (ADH)[1] stimulates transepithelial water flow across amphibian skin and urinary bladder by causing the insertion of particle aggregates in the apical membranes of principal cells, reviewed recently by Handler (1988). The aggregates are thought to constitute the putative "water channel" (Harris and Handler, 1988) with a pore size so small ($2\mathring{A}$) as to preclude the entry of small solutes, but sufficient to permit proton permeation in the form of hydronium ions or possibly by a Grotthus conductance effect (see Glasstone and Lewis, 1960; Stein, 1986), by which protons are passed on between neighboring hydrogen-bonded water molecules. A high membrane proton conductance is indicative, therefore, of a water-filled channel. The demonstration that vasopressin increases proton conductance in toad urinary bladder has provided the strongest evidence to date that ADH increases water permeability by inducing aqueous-filled pores in the apical cell membranes (Gluck and Al-Awqati, 1980).

Recently, it has been suggested that, besides conducting protons, the water channel may be similar to the F_o ($F_{oligomycin}$) component of the F_1-F_o class of H^+-adenosine triphosphatase (ATPase) (Harris and Handler, 1988). The F_o complex forms a narrow

[1] ADH is synonymous for vasopressin, arginine vasotocin, and oxytocin.

membrane-spanning pore which will only allow the passage of water and protons (Senior and Wise, 1983) and binds dicyclohexylcarbodiimide (DCCD) and oligomycin. Here we have tested the hypothesis that water flows across the apical cell membranes through proton permeable channels, which have possibly evolved from an F_o protein, by comparing the effects of oxytocin on water flux and H^+ conductance and their response to known inhibitors of mitochondrial and epithelial classes of F_1-F_o H^+-ATPase.

Although much insight has been gained into water transport phenomena from studies of ADH-induced morphological and permeability changes at the apical membrane, little is known in comparison about the water transport pathway across the basolateral cell membrane. Since ADH-induced water flow is transcellular, the native water permeability of the basolateral cell membranes must either be spontaneously high or be increased by ADH in a manner different from that at the apical cell membrane. The high water permeability of this membrane (MacRobbie and Ussing, 1961; Strange and Spring, 1987) points to the presence of aqueous-filled pores rather than increased lipid fluidity. Here we have tested the possibility that water crosses the basolateral cell membranes via pores by determining the proton conductance of this membrane and its sensitivity to inhibitors of water transport, and in turn, the response of net water flow to blockers of H^+ conductance.

Besides using proton conductance as an indicator of water-permeable pores, there may be a possible role for H^+ per se in the regulation of ADH-induced water flux. There is evidence that ADH produces a fall in intracellular pH about the time of the peak hydroosmotic response (Brem et al., 1986) and that fluctuations in pH_i may in some way be involved in the regulation of water transport (Carvounis et al., 1979; Parisi et al., 1983; Parisi and Bourguet, 1984; Brem et al., 1985). These effects of pH_i on water permeability take on added significance if it can be shown that water and protons share a common pathway and if their permeability can be simultaneously affected by ADH.

A preliminary account of this work has been presented (Harvey et al., 1989).

METHODS

The experiments were performed on the isolated epithelium of *Rana esculenta* ventral skin and on the isolated urinary bladder sac preparation from the same frog species (supplied by Couetard, St. Hilaire de Riez, France and originating from Yugoslavia). The animals were adapted to running tap water at 15°C. The techniques for isolation of the skin epithelium using collagenase (1 mg/ml, class II Worthington Biochemical Corp., St. Louis, MO) and for mounting and perfusion of the tissue in Ussing-type chambers (DCDV, Saint Lyé la Forêt, France) have been described previously (Harvey et al., 1988). The epithelium was normally superfused on both sides with a Ringer solution designated "control" which had the following composition (in millimolar) NaCl 105, KCl 2.5, $CaCl_2$ 2, $MgCl_2$ 2, KH_2PO_4 2.5, glucose 11, equilibrated in air and buffered to pH 7.4 with 10 mM N,N-bis-(2-hydroxyethyl)-2-amino-ethansulfonate BES. Ringer solutions of similar ionic composition to control but of different pH were prepared by substituting BES by the following buffers (10 mM): N-[2-hydroxy-1,1-bis(hydroxymethyl)-ethyl]glycine (TRICINE) for pH 8.2 and 2-morpholinoethansulfonate (MES) for pH 6.4, 5.5, 4.4, and 3.4. The solutions were titrated to the required pH with either 1 N NaOH or HCl. In some experiments, the control Ringer solution was gassed with 5% CO_2 in O_2, to produce a pH between 6.2 and 6.4 ("CO_2 Ringer"). Amiloride was purchased from

Merck Sharp & Dohme, West Point, PA. Diethylstilbestrol (DES), 4,4'di-isothiocyanostilbene 2-2'disulfonic acid (DIDS), DCCD, N-ethylmaleimide (NEM), vanadate, and verapamil were purchased from Sigma Chemical Co, St. Louis, MO. Diphenylamine carboxylate (DPC) was purchased from Fluka, Buchs, Switzerland. Oligomycin and ethylisopropylamiloride (EIPA) were gifts from Aldrich Chemical Co., Milwaukee, WI, and from Dr. E. J. Cragoe, Merck Sharp & Dohme, respectively.

Microelectrodes

We used the isolated skin epithelium for the microelectrode studies on H^+ permeation since this tissue, compared with the urinary bladder, affords a much easier technical approach using double-barreled pH-sensitive microelectrodes. All the microelectrode experiments were carried out under short-circuit conditions when the spontaneous transepithelial electrical potential difference (V_t) was clamped at 0 V using an automatic voltage clamp (model VC600, Physiologic Instruments, Houston, TX). Intracellular pH was measured using double-barreled H^+-sensitive microelectrodes containing proton-selective liquid ion exchanger (proton cocktail 82500, Fluka; Amman et al., 1981) coupled to a dual-microprobe amplifier (model FD223, World Precision Instruments, Inc., New Haven, CT). Their construction and calibration and methods used to simultaneously measure pH_i, cell membrane current–voltage $(I-V)$ relations, and conductances have been described in detail (Harvey et al., 1988; Harvey and Ehrenfeld, 1988a). In some experiments, membrane potentials and $I-V$ relations were recorded with single-barreled conventional microelectrodes (filled with 1 M KCl), coupled to a dual-microprobe amplifier (model 750, World Precision Instruments, Inc.). The $I-V$ relations were generated automatically by the VC600 amplifier under computer command while V_t was clamped between +100 and −100 mV in 20-mV incremental bipolar steps and maintained at each value for a duration of 210 ms with an interval of 50 ms between pulses. The apical and basolateral $I-V$ data were sampled at 8 and 200 ms, respectively, during the pulse period. The longer pulse duration for the basolateral membrane voltage clamp is required for the dissipation of capacitative transients. Slope conductances were calculated at 5-s intervals and values interpolated to give a quasi-continuous readout of apical and basolateral cell membrane conductances.

The outputs from the amplifiers VC600, WPI 750, and FD223 were recorded on an oscilloscope (model 5115, Tektronix, Inc., Beaverton OR), a potentiometric pen recorder (model 2065, Linseis, FRG), and digitized via a 16-bit analog/digital converter for computer storage and processing using a UNISOFT program (H. Gross, CA). The voltage clamp was run using custom-built software which performed fitting of Goldman-Hodgkin-Katz (GHK) equations to $I-V$ data to yield estimates of membrane permeability and slope conductance. In some experiments an equivalent circuit analysis was made of cell membrane conductances and electromotive force using measurements of the fractional resistance (FR_a) of the apical cell membranes (Harvey and Kernan, 1984). The response of FR_a to amiloride block of Na^+ channels, the fit of the GHK equation to amiloride-sensitive apical Na^+ channel $I-V$ relations and the stability of electrode tip resistance, were used as criteria for successful microelectrode impalement of the cells.

Net Water Flow and Titratable H^+ Flux

Transepithelial net water fluxes were measured across urinary bladder sacs of the same frog species used in the electrophysiological studies. Although R. esculenta skin increases its water permeability over 25-fold in response to ADH (Maetz, 1968) we preferred to use the urinary bladder in the hydroosmotic studies because of its greater response to ADH, the relative ease in

measuring net water flow using the sac technique, and its well-documented and recognized role as a model epithelium in ADH studies.

Bladder sacs were prepared by first thoroughly flushing and filling each bladder in situ with half-strength Ringer solution to almost maximum capacity (~12 ml). After isolation, the bladder sacs were incubated at room temperature in beakers containing half-strength Ringer solution with oxytocin (50 mU/ml). Water flux was measured at 5–10-min intervals from the change in weight of the bladder sac over a 20–30-min period. After this equilibration period one bladder sac was plunged into a beaker containing full-strength Ringers solution with oxytocin (control) while its experimental pair was placed in a similar solution containing the agent to be tested (for serosal effects) or inhibitor was added directly to the luminal solution via a catheter (for apical effects).

Titratable H^+ net fluxes (J_{H^+}) were measured across frog skin and urinary bladder sacs using a fixed end-point titration technique previously described in detail (Ehrenfeld et al., 1985). J_{H^+} was determined at 15-min intervals by calculating the change in titratable acidity in 2-ml samples of serosal or apical bathing solutions for bladder or skin experiments, respectively. In experiments where net water flow and net H^+ flux were monitored simultaneously, the bladders were exposed to combined transepithelial hydroosmotic and pH gradients (lumen pH 5.5, serosal pH 7.4: half-strength Ringer in lumen and normal Ringer solutions on serosal side). Fluxes are expressed per square centimeter of luminal surface area calculated from the volume of the bladder sac sphere (estimate radius from volume $V = \frac{4}{3}\pi r^3$ and surface area from $S = 3V/r$).

Data are presented as mean ± SEM.

RESULTS

Native H^+ Permeability of the Apical Membranes of Isolated Frog Skin Epithelium

The H^+ permeability of apical cell membranes of principal cells in frog skin, under short-circuit and spontaneous Na^+ transport conditions, was assessed in the absence of oxytocin by monitoring intracellular pH when the pH of the apical bathing solution (pH$_a$) was changed over the range 7.4–3.4. A typical experiment in Fig. 1 *A* demonstrates that lowering pH$_a$ in the absence of oxytocin was accompanied by a fall in membrane conductances and an intracellular acidification. The decrease in apical and basolateral membrane conductances and inhibition of short-circuit current reflect the block of apical Na^+ channels and basolateral K^+ channels by intracellular protons (Harvey et al., 1988). When the external pH was lowered in the presence of amiloride (50 μM apical side), pH$_i$ showed negligible variations in response to lowering external pH (Fig. 1 *B*), even at pH$_a$ 3.4. The amiloride-sensitive intracellular acidification at low pH$_a$ indicates that Na^+ channels are permeable to protons (Harvey and Ehrenfeld, 1986). The ratio of Na^+ and H^+ permeabilities calculated from the GHK equation fit to amiloride-sensitive *I-V* relations indicates that at pH$_a$ 5.5 proton and sodium permeabilities are about equal, whereas at pH$_a$ = 3.4, hydrogen ions are six times more permeant than Na^+, which is in agreement with permeability ratios reported for toad urinary bladder (Palmer, 1982).

Effect of Oxytocin on H^+ Permeation across the Apical Membrane

ADH is known to increase apical Na^+ permeability (Macknight et al., 1980), and we routinely blocked this pathway with micromolar concentrations of amiloride to obtain

a low resting proton permeability and to distinguish between an eventual proton flux through ADH-activated Na⁺ channels and water channels. This protocol appears valid since we found that amiloride does not block oxytocin effects on H^+ permeability and the diuretic does not affect the hydroosmotic water response (Parisi et al., 1983). Oxytocin has also been shown to activate apical Ca^{2+} channels, but these are
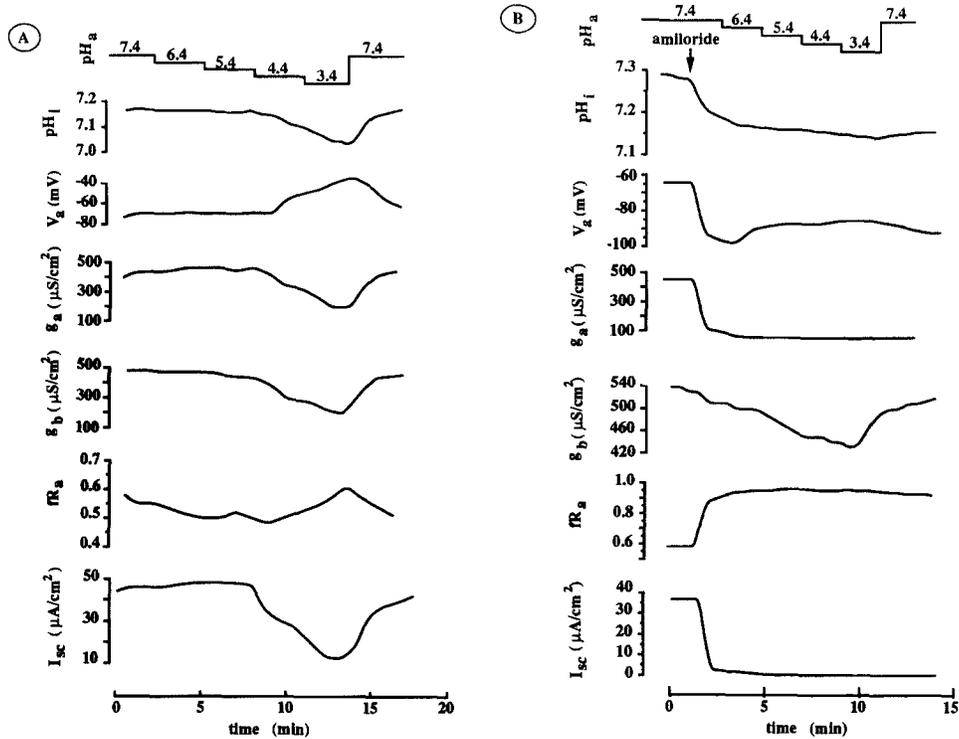
FIGURE 1. Double-barreled H^+-sensitive microelectrode recording of the effects of apical solution pH on intracellular pH, membrane potential and conductances in principal cells of isolated short-circuited epithelium from *Rana esculenta* skin under conditions of (*A*) spontaneous sodium transport and (*B*) after block of Na⁺ transport by amiloride (50 μM). The variations in conductances and current in *A* result from pH_i effects on apical Na⁺ and basolateral K⁺ conductances, and in *B* are due to amiloride block of apical Na⁺ channels and residual pH_i effects on basolateral K⁺ channels.

not spontaneously open at physiological concentrations of Ca^{2+} and are blocked by low pH (Van Driessche and Zeiske, 1985; Van Dreissche, 1987).

Oxytocin (50 mU/ml basolateral side) produced a gradual intracellular acidification at pH_a 7.4, which reached a maximum after ~10 min. Apical application of oxytocin was without effect on pH_i, membrane potential, and conductance. Unlike the situation without hormone, the intracellular pH became very sensitive to changes in pH_a after ADH treatment and a rapid and reversible intracellular acidification was

observed when external pH was lowered to 6.4 and 5.5 (Fig. 2 *A*). ADH-stimulated H$^+$ flux across the apical membrane is electrogenic and can be influenced by membrane potential. Voltage clamping the apical membrane to more negative potentials (−100 mV) produced a further fall in pH$_i$ accompanied by an increase in apical membrane conductance (Fig. 2, *A* and *B*).

In ADH-treated epithelia the electrochemical driving force for H$^+$ (μH^+) transport across the apical cell membranes favors passive influx of H$^+$ at external pH < 7.4
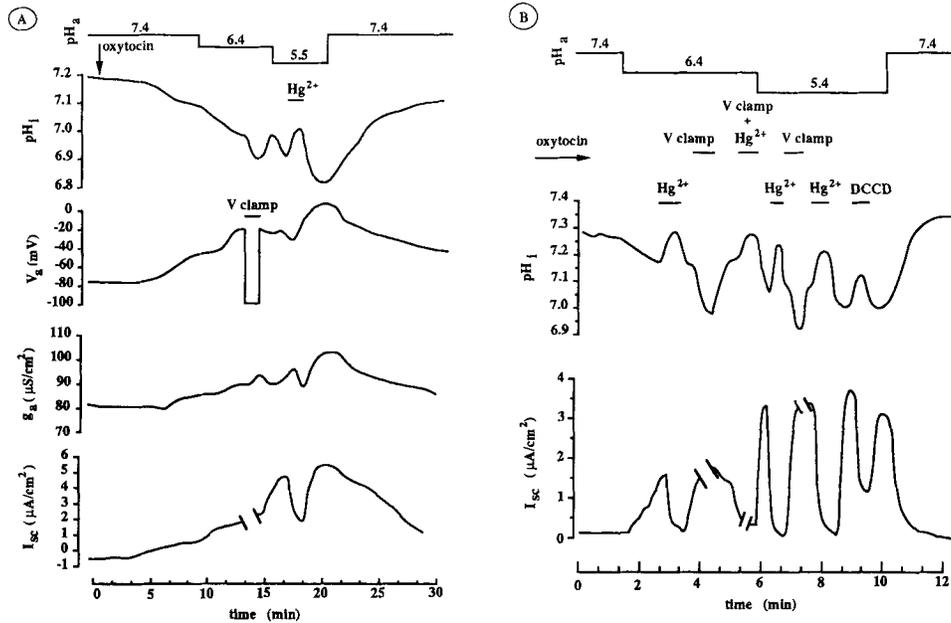
FIGURE 2.   Effects of oxytocin on intracellular pH of a principal cell at various external apical pH values in a short-circuited isolated frog skin pretreated with amiloride (50 μM apical side). Decreasing external pH from 7.4 to 6.4 and 5.4 produced a rapid voltage-sensitive fall in pH$_i$ and an increase in short-circuit current which were blocked by addition of Hg^{2+} (100 μM) or dicyclohexylcarbodiimide (DCCD, 10^{-5} M) to the apical bath. In *A*, oxytocin was added to the serosal bath at arrow and in *B*, the epithelium was exposed to oxytocin for 20 min before the onset of the record. At bars marked *V clamp*, a transepithelial current pulse was passed to voltage clamp the apical membrane at −100 mV.

(Table I) and the μH^+ across the basolateral cell membranes favors H$^+$ efflux into the serosal bath (Table I). Thus passive transcellular H$^+$ flux is directed from apical to basolateral side at all pH$_a$ below 7.4. Under such conditions, lowering external pH produced a transepithelial current (Fig. 2, *A* and *B*) and stimulated an equivalent transepithelial titratable J_{H^+} (Table I). For example, at pH$_a$ 4.5, J_{H^+} = 165 neq·h^{-1}·cm^{-2}, equivalent to 4.4 μA·cm^{-2}, which is in close agreement with the measured short-circuit current (I_{sc}) (4.5 μA·cm^{-2}). The equivalence between J_{H^+} and I_{sc} implies that protons are the sole charge carrier of the ADH-activated current.

TABLE I

Conductances, Permeabilities, and Electrochemical Driving Forces for H^+ across Apical and Basolateral Cell Membranes of Oxytocin-treated Frog Skin Epithelia Measured at Different Apical Bathing Solution pH

pH_o	pH_i	E_H^a	μ_H^a	E_H^b	μ_H^b	g^a	g_H^a	I_H^a	p_H^a	E_H^T	J_H^a	K_{trans}
		mV	mV	mV	mV	$\mu S \cdot cm^{-2}$		$\mu A \cdot cm^{-2}$	$10^{-3} \cdot cm \cdot s^{-1}$	mV	$neq \cdot h^{-1} \cdot cm^{-2}$ ($\mu A \cdot cm^{-2}$)	$10^{-3} cm \cdot s^{-1}$
7.4 (n = 8)	7.10 ± 0.04	−17 ± 3	+38 ± 3	−17 ± 3	+38 ± 3	85 ± 10	5 ± 2	0.10 ± 0.05	1.24 ± 0.3	−8 ± 2	—	—
6.4 (n = 8)	6.95 ± 0.03	34 ± 4	54 ± 5	−26 ± 3	−6 ± 1	94 ± 10	12 ± 3	2.0 ± 0.10	5.9 ± 0.8	27 ± 4	—	—
5.5 (n = 8)	6.80 ± 0.02	75 ± 7	80 ± 8	−34 ± 3	−29 ± 4	110 ± 18	30 ± 3	3.2 ± 0.2	2.2 ± 0.3	82 ± 10	118 ± 37 (3.2)	3.07
4.5 (n = 8)	6.65 ± 0.05	125 ± 4	115 ± 8	−44 ± 4	−34 ± 4	130 ± 17	45 ± 5	4.5 ± 0.3	0.70 ± 0.1	120 ± 15	165 ± 28 (4.4)	1.05

Apical membrane H^+ slope conductance, current, and permeability were calculated from Hg^{2+}-sensitive current-voltage relations of apical cell membranes. E_H^a and E_H^b are the measured Nernst potentials for H^+ across apical and basolateral cell membranes, respectively. μ_H^a and μ_H^b are the H^+ electrochemical driving forces; positive values denote H^+ influx, negative values H^+ efflux; g^a total apical membrane slope conductance; g_H^a, I_H^a, p_H^a, and E_H^T are Hg^{2+}-sensitive H^+ slope conductance, current, permeability, and reversal potentials, respectively, calculated from GHK equation fits to I-V data. Net titrametric H^+ fluxes (J_H^a) are given with the equivalent current in parentheses.

Apparent proton permeability (K_{trans}) was calculated from $J_H^a / 10^{-pH_a}$.

Inhibition of ADH-induced H⁺ Permeability

The effects of low external pH on pH_i, g_a and I_{sc} were halted by adding 100 μM $HgCl_2$ to the apical solution (Fig. 2, A and B). Furthermore, Hg^{2+} prevented the fall in pH_i normally produced by a hyperpolarizing voltage clamp (Fig. 2 B). Other mercury-containing agents such as micromolar concentrations of *p*-chloromer-curibenzenesulfonate (pCMBS) had similar effects as Hg^{2+}. The sensitivity of ADH-induced proton permeability to mercurials is interesting in that mercurial compounds have been recently shown to block ADH-induced water flux in frog urinary bladder by a direct interaction with the water channel (Ibarra et al., 1989).

DCCD, an inhibitor of H^+ flux through reconstituted F_o channels (Nelson, 1981; Sebald et al., 1982), blocked the ADH-stimulated H^+ permeability and inhibited I_{sc}
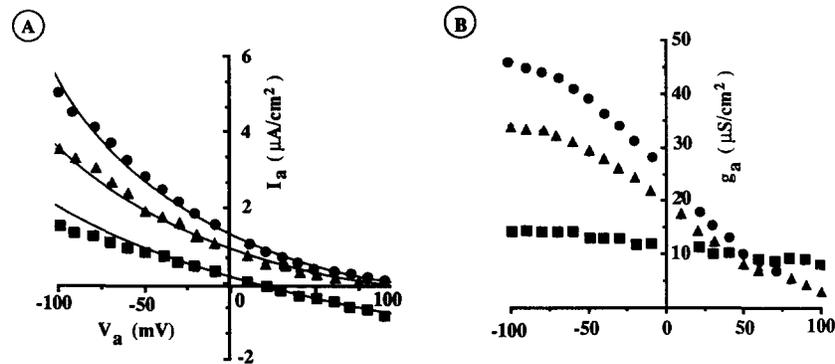
FIGURE 3. Mercury-inhibitable (A) current–voltage relations and (B) slope conductance of apical membranes of principal cells recorded at three different external apical pH values: (●) pH_a 4.5; (▲) pH_a 5.5; (■) pH_a 6.4 in oxytocin-treated frog skin epithelia (in the presence of amiloride to block apical Na^+ channels). The solid lines represent the fit of the GHK equation to the data. Reversal potentials were in good agreement with measured Nernst potentials for H^+ across the apical membrane. The apparent proton permeability coefficients, conductances and reversal potentials obtained from the GHK fit are given in Table I.

when added to the apical solution (Fig. 2 B). The effect of short-term exposure (<30s) to DCCD (10^{-5} M) was rapid and reversible and was observed only with apical addition, serosal DCCD was without effect. Longer periods of exposure to DCCD (>60 s) produced irreversible inhibition of I_{sc} and failure of low pH_a to induce intracellular acidification.

The low proton permeability of the apical cell membranes in unstimulated epithelia was confirmed by measurements of net titratable acid flux across 12 isolated frog skins exposed to pH_a 5.5. In the absence of ADH the net transepithelial H^+ flux was very low (30 ± 5 neq·h⁻¹·cm⁻²). Exposure to oxytocin had a marked stimulatory effect on J_{H^+} (115 ± 18 neq·h⁻¹·cm⁻²), which was completely and irreversibly inhibited (34 ± 3 neq·h⁻¹·cm⁻²) after 15 min of exposure to apical DCCD (10^{-5} M).

Proton Current–Voltage Relations

Hg^{2+} completely and reversibly blocks the oxytocin-induced H^+ current and we used it to extract apical membrane proton current-voltage relations. Fig. 3, A and B shows

mercury-sensitive I-V relations and slope conductances of the apical membrane at three different pH_a values determined 30 min after oxytocin was added to the serosal bath. The measured pH_i and membrane current values were used to solve a GHK equation fit to the I-V data. The best fit equation yielded values of apparent proton permeability which agree with H^+ permeability coefficients (K_{trans}) determined from titratable H^+ flux experiments[2] (Table I). The Hg^{2+}-sensitive I-V relations accurately describe electrogenic H^+ transport across the apical cell membranes. The reversal potentials are close to the measured Nernst potential for H^+ (E_H) across this membrane. The Hg^{2+}-sensitive H^+ current and slope conductance are comparable to the changes in total transepithelial current, titratable H^+ flux, and membrane conductance at similar pH_a (Table I).

H^+ Permeability of the Basolateral Cell Membranes

The permeability of the basolateral membrane to protons was investigated by measuring intracellular pH in isolated epithelia as a function of the pH of the basolateral bathing solution (pH_b). Principal cells were punctured from the basolateral side with double-barreled H^+-sensitive microelectrodes in epithelia treated with apical amiloride (50 μM) to inhibit the transepithelial Na^+ current. We found that the basolateral cell membranes are spontaneously permeable to H^+. Lowering pH_b in the absence of oxytocin produced an immediate intracellular acidification and membrane depolarization which were reversible on removal of the external acid load (Fig. 4). The changes in membrane potential result mainly from an inhibition of K^+ conductance at low pH_i (Harvey et al., 1988). The intracellular acidification response to lowering pH_b was unchanged in the presence of oxytocin (Fig. 5). From a comparison of the relationship between pH_i and pH_a or pH_b, it appears that the proton permeability of the basolateral cell membranes in unstimulated tissues matches that of the apical membranes in hormone-treated epithelia (Fig. 5 and Tables I and II).

Effect of Heavy Metals on H^+ Permeation

The changes in pH_i induced by low pH_b (5.5) were found to be insensitive to a wide range of inhibitors of ionic channels, exchangers, and cotransporters when applied to the basolateral side at concentrations which inhibit these systems in epithelial tissues. We tested a variety of agents which turned out to have no effect on acid-induced membrane depolarization or intracellular acidification, such as inhibitors of Na^+ channels (amiloride 10^{-5} M), K^+ channels (barium 10^{-3} M), Cl^- channels (DPC 10^{-6} M), Ca^{2+} and nonselective cation channels (van Driessche and Zeiske, 1985) (verapamil 10^{-6} M), Na^+/HCO_3^- cotransport or Cl^-/HCO_3^- exchange (DIDS 10^{-5} M), Na^+/H^+ exchange (EIPA 10^{-5} M), vacuolar type H^+ ATPase (NEM 10^{-4} M), mitochondrial F_1-F_o type H^+ ATPase (oligomycin 10^{-6} M), H^+/K^+ ATPase (vanadate 10^{-5} M) and Na^+/K^+ ATPase (ouabain 10^{-4} M). The change in pH_i at low pH_b was also insensitive to inhibition of mitochondrial respiration (cyanide 10^{-5} M) or to blockers of carbonic anhydrase (ethoxzolamide 10^{-5} M).

---

[2] Both methods reveal an inverse relationship between proton permeability and external H^+ activity reminiscent of a similar relationship between external Na^+ and its permeability (Harvey and Kernan, 1984). Possibly, like Na channels, the proton site is autoregulated.
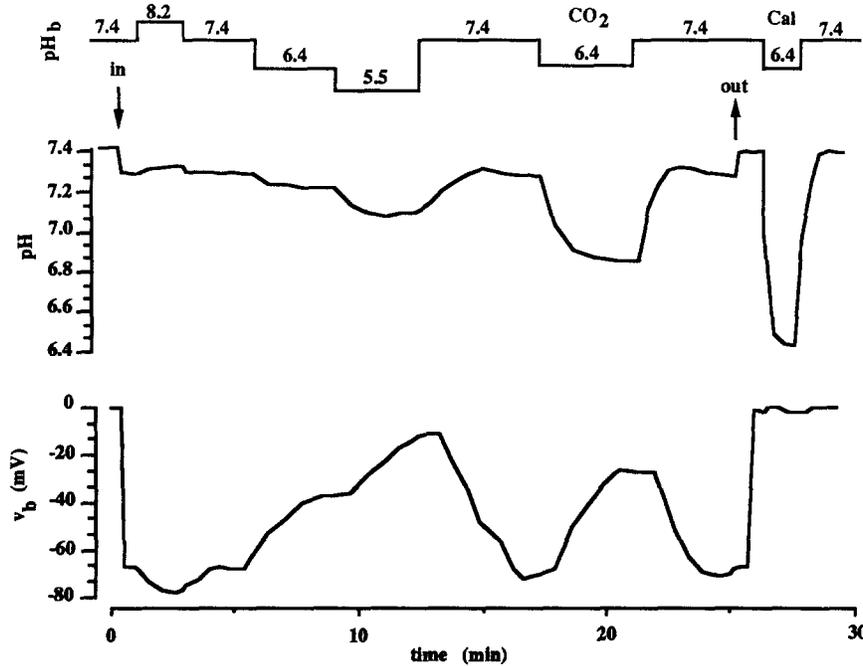
FIGURE 4. Recording of the effects of changing basolateral solution pH on intracellular pH and membrane potential measured with a double-barreled H^+-sensitive microelectrode in a principal cell of an isolated epithelium under short-circuit conditions. Impalement from the basolateral side is marked by the arrow "in." In the right-hand side of the record pH_b was varied between 8.2 and 5.5 using nonpermeant buffers. The pH_i decreased with external acidification, indicating that the basolateral cell membranes are spontaneously permeable to H^+. For comparison, the effect of a permeant weak acid (5% CO_2 in HCO_3^- free Ringer, pH_b 6.4) on pH_i and V_b is also shown. The electrode was withdrawn from the cell into the basolateral solution (at arrow "out") and calibrated in solutions pH_b 7.4 and 6.4.
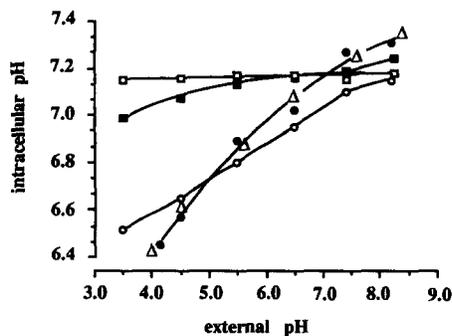
FIGURE 5. Relationship between intracellular pH and external apical or serosal pH in amiloride and oxytocin treated epithelia. Effects of changing apical pH in spontaneous Na transporting epithelia (■ [n = 5]), amiloride-treated epithelia (□ [n = 8]), and amiloride plus oxytocin-treated epithelia (○ [n = 8]). Effects of changing serosal pH in amiloride-treated epithelia (● [n = 8]), and amiloride plus oxytocin-treated epithelia (△ [n = 8]).

In excitable tissues, H^+ currents are blocked by heavy metals (Thomas, 1988) and we tested the effects of Hg^{2+}, Zn^{2+}, Ni^{2+}, Cd^{2+}, and Co^{2+} on the voltage and pH_i response to a rapid change in pH_b between 7.4 and 5.5 in amiloride-treated epithelia. When present at 100 μM in the basolateral solution, the heavy metals were effective in partially repolarizing the membrane potential and fully reversed the intracellular acidification induced at low pH_b (Fig. 6A), half-maximal recovery of pH_i was produced at 17.5 μM $[Zn^{2+}]$ at a pH_b 5.5. Prior application of Ni^{2+} to the basolateral solution also prevented the intracellular acidification at low pH_b (Fig. 6B) and subsequent removal of Ni^{2+} at low external pH gave rise to an intracellular acidification. The effects of the heavy metals on basolateral membrane potential (V_b) and pH_i were rapid and fully reversible, indicating an external rather than an intracellular site of action (their addition to the apical solution at 100 μM had no effect on V_b or pH_i).

TABLE II

Conductances, Permeability, and Electrochemical Driving Forces for H^+ across Basolateral Cell Membranes of Oxytocin-treated Frog Skin Epithelia Measured at Different Basolateral Bathing Solution pH

pH_b	pH_i	E_H^b	μ_H^b	g^b	g_H^b	I_H^b	P_H^b	E_H^r
		mV	mV	$\mu s \cdot cm^{-2}$		$\mu A \cdot cm^{-2}$	$10^{-3} cm \cdot s^{-1}$	mV
8.2 (n = 8)	7.31 ± 0.07	−52 ± 5	40 ± 5	769 ± 110	0.40 ± 0.11	0.01 ± 0.01	1.8 ± 0.2	−50 ± 4
7.4 (n = 8)	7.27 ± 0.04	−8 ± 1	72 ± 6	611 ± 82	7.88 ± 0.90	0.15 ± 0.05	3.9 ± 0.3	−7 ± 2
6.4 (n = 8)	7.02 ± 0.06	46 ± 5	96 ± 11	194 ± 44	46.5 ± 5.0	1.17 ± 0.22	3.1 ± 0.3	40 ± 5
5.5 (n = 8)	6.89 ± 0.05	81 ± 10	91 ± 10	35 ± 10	171 ± 20	4.41 ± 0.53	1.5 ± 0.2	88 ± 12
4.5 (n = 8)	6.57 ± 0.04	120 ± 13	130 ± 14	12 ± 5	341 ± 35	10.1 ± 0.98	0.3 ± 0.1	113 ± 15

Basolateral cell membrane H^+ slope conductance, current, and permeability were calculated from Zn^{2+}-sensitive current voltage relations. E_H^b is the measured Nernst potential for H^+; μ_H^b the H^+ electrochemical driving force; g^b total basolateral membrane slope conductance; and g_H^b, I_H^b, P_H^b, and E_H^r are Zn^{2+}-sensitive H^+ slope conductance, current, permeability, and reversal potentials, respectively, calculated from GHK equation fits to the I-V data.

Part of the membrane potential response to low pH_b must involve a decrease in basolateral membrane K^+ conductance since K channels are very sensitive to changes in pH_i (Harvey et al., 1988). We therefore tested the effects of heavy metals and acidic external solutions on pH_i and V_b when the spontaneous K^+ conductance of the basolateral membranes was blocked by Ba^{2+} (Fig. 7). In addition to monitoring pH_i and V_b, the K^+ transference (t_K) of the basolateral cell membranes was determined from the response of V_b to raising extracellular $[K^+]$ from 3.7 to 37 mM. The blocking effect of H^+ on K^+ conductance was apparent from the reduction in t_K at low external pH (t_K = 0.97 ± 0.02 at pH_b 7.4, t_K = 0.38 ± 0.02 at pH_b 6.4, and t_K = 0.07 ± 0.01 at pH_b 5.5, n = 24). Ba^{2+} (1 mM) completely blocked K^+ conductance at pH_b 7.4 (t_K = 0.015 ± 0.005, n = 8) and at pH_b 5.5 (t_K = 0.014 ± 0.007, n = 4). Ba^{2+} did not prevent the fall in pH_i at low pH_b. Lowering pH_b in the presence of Ba^{2+} produced an increase in basolateral membrane conductance and this effect,

including the fall in pH_i, were reversed when Zn^{2+} (100 μM) was added to the basolateral solution. This effect of zinc does not involve K^+ conductance since the t_K in barium-containing Ringer solutions at pH_b 5.5 was the same whether Zn^{2+} was present (t_K = 0.012 $\pm$ 0.001, n = 4) or absent (t_K = 0.015 $\pm$ 0.005, n = 4). Furthermore, micromolar concentrations of heavy metals when added alone in the absence of Ba^{2+} had no effect on K^+ conductance nor did they interfere with block of K^+conductance by Ba^{2+} at pH_b 7.4. These data indicate that a heavy metal–sensitive rheogenic H^+ permeation pathway is present in basolateral cell membranes.
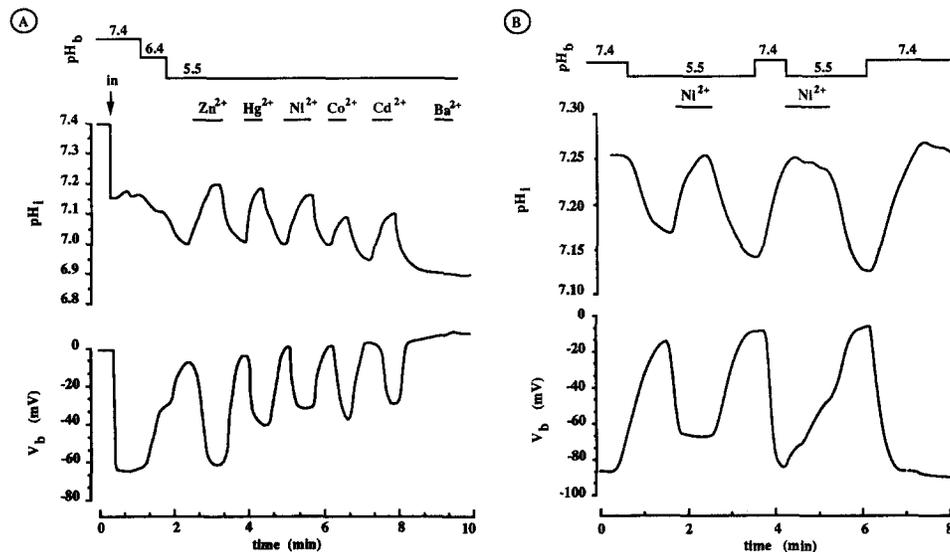
FIGURE 6.   Double-barreled H^+-sensitive microelectrode recording of pH_i and V_b after cell penetration from the basolateral side (arrow "in"). (A) Effects of heavy metals added at 100 μM to the basolateral solution on intracellular acidification and membrane depolarization induced at low extracellular pH_b 5.5. (A) Zn^{2+}, Hg^{2+}, Ni^{2+}, Co^{2+} and Cd^{2+} were effective in reversing the fall in pH_i and produced partial recovery of the membrane potential. Unlike the heavy metals, Ba^{2+} had no effect on pH_i and since V_b was also unaffected this indicates that K^+ conductance is completely blocked at pH_b 5.5 and pH_i 6.9. (B) Effect of 100 μM $NiCl_2$ on pH_i and V_b at extracellular pH_b 5.5. Addition of Ni^{2+} to the basolateral bath reverses the fall in pH_i at low pH_b, while addition of Ni^{2+} before changing pH_b largely prevented the decrease in pH_i at pH_b 5.5.

Transepithelial Currents Induced by Oxytocin at Low pH_b

Although lowering pH_b was associated with the appearance of a heavy metal-sensitive inward current (inferred from membrane depolarization and increased conductance in the presence of Ba^{2+}), there was no change in transepithelial short-circuit current in amiloride and Ba^{2+}-treated epithelia. When such epithelia were incubated for a minimum of 10 min with oxytocin (50 mU/ml basolateral side), lowering pH_b induced a basolateral to apical-directed transepithelial current which was inhibited by the addition of micromolar concentrations of the heavy metals on the basolateral side

and by DCCD from the apical side (Fig. 8 A). The transepithelial proton-dependent current was found to be very sensitive to basolateral [Zn^{2+}]. At pH_b 5.5, half-maximal inhibition of the proton current was produced at 20 μM Zn^{2+}. As was shown in Fig. 2, A and B, a proton-dependent current could also be driven in the apical to serosal direction in oxytocin-treated epithelia exposed to a suitable transepithelial pH gradient (pH_a 5.5 or 4.5/pH_b 7.4), this current was reversibly blocked by heavy metals and micromolar concentrations of pCMBS (not shown) from the basolateral side (Fig. 8 B).
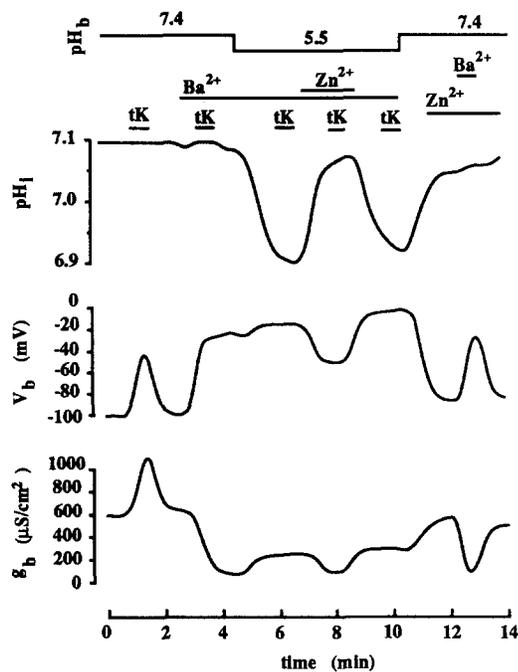
FIGURE 7. Recording of intracellular pH, basolateral membrane potential and conductance as a function of extracellular pH in the presence of Ba^{2+} (1 mM) and/or Zn^{2+} (100 μM). The partial conductance of the basolateral cell membranes to K^+ is reflected in the measurement of K^+ transference (tK) (the response of V_b to increasing extracellular [K^+] from 3.7 to 37 mM during bars marked tK). Ba^{2+} completely blocked K^+ conductance without affecting the steady-state pH_i. Lowering pH_b in the presence of Ba^{2+} produced a fall in pH_i and an increase in membrane conductance and these effects were reversed by Zn^{2+}. Addition of Zn^{2+} at pH_b 7.4 had no effect on pH_i (nor on tK) and did not interfere with Ba^{2+} inhibition of K^+ conductance.

Current–Voltage Relations of Zn^{2+}-sensitive Proton Permeation

Since Zn^{2+} blocks transepithelial proton currents induced by oxytocin at low pH_b, we used it as a chemical tool to extract proton-dependent I-V relations of the basolateral cell membranes. The Zn^{2+}-sensitive I-V relations and slope conductances recorded as a function of pH_b are given in Fig. 9, A and B. The reversal potentials are similar to the measured E_H across this membrane at all pH_b (Table II). Furthermore, the effects of pH_b on Zn^{2+}-sensitive current and conductance agree with the actual measured changes in these membrane electrical parameters. Thus, the Zn^{2+}-sensitive I-V relations accurately describe electrodiffusional H^+ transport across the basolateral membranes. The apparent H^+ permeability coefficients and slope conductance calculated from a GHK equation fit to Zn^{2+}-sensitive I-V relations are given in Table
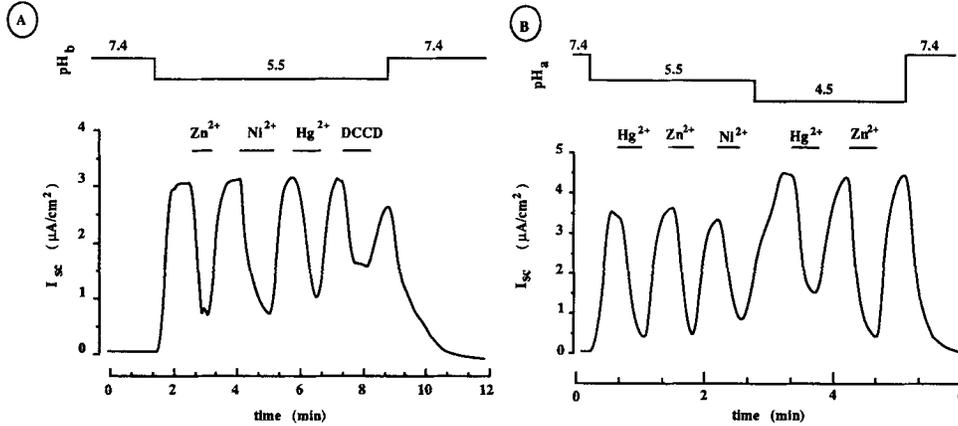
FIGURE 8. Response of short-circuit current to external pH changes in isolated epithelia treated with amiloride (10^{-5} M apical side) and oxytocin (50 mU/ml basolateral side). (*A*) Effects of heavy metals (100 μM basolateral side) and dicyclohexylcarbodiimide (DCCD, 10^{-5} M apical side) on the transepithelial basolateral to apical-directed current induced by lowering basolateral solution pH to 5.5. (*B*) Effects of heavy metals (100 μM basolateral side) on apical to basolateral-directed transepithelial current induced at low apical pH.

II. The basolateral membrane H^+ permeability is high and matches the ADH-stimulated apical proton permeability at equivalent external pH (compare with Table I).

Oxytocin-activated Hydroosmotic Water Flow: Effects of Inhibitors of H^+ Transport

If water and protons share a common channel at apical and basolateral cell membranes, then this should be revealed by a comparison between the effects of oxytocin and inhibitors on net water flow and rheogenic H^+ flux. Oxytocin did not
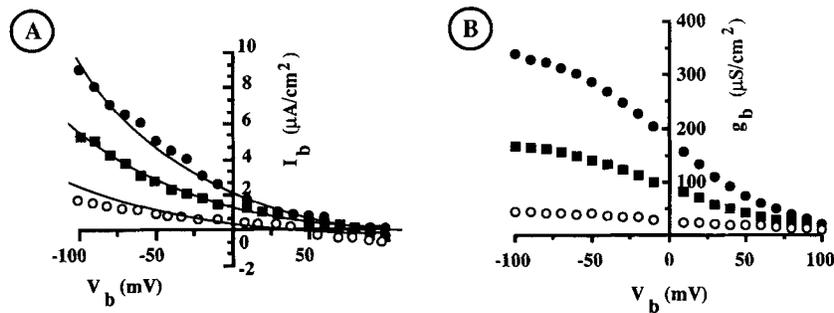
FIGURE 9. Zn^{2+}-sensitive (*A*) current–voltage relations and (*B*) slope conductance of basolateral cell membranes in isolated epithelia treated with amiloride (50 μM apical side), and basolateral Ba^{2+} (1 mM) and oxytocin (50 mU/ml) at different basolateral solution pH: (●) pH_b 4.5; (■) pH_b 5.5; (○) pH_b 6.4. Solid lines are a GHK equation fit to the *I-V* data. Values for apparent H^+ permeability coefficients, conductances and reversal potentials are given in Table II.

affect net water flow under isotonic conditions and during this time the hormone triggers cAMP-dependent events which cause the incorporation of particle aggregates into the apical membranes (Chevalier et al., 1970). The neccessary transport machinery is in place to support hydroosmotic water flow (J_{H_2O}) and a sudden osmotic shock (luminal side hypotonic relative to the serosal bath) produced an immediate increase in (J_{H_2O}), which reached a maximum value after 10–20 min and then declined over a period of 60–90 min, stabilizing at values more elevated than untreated controls (Fig. 10 A). This procedure of preincubation with oxytocin
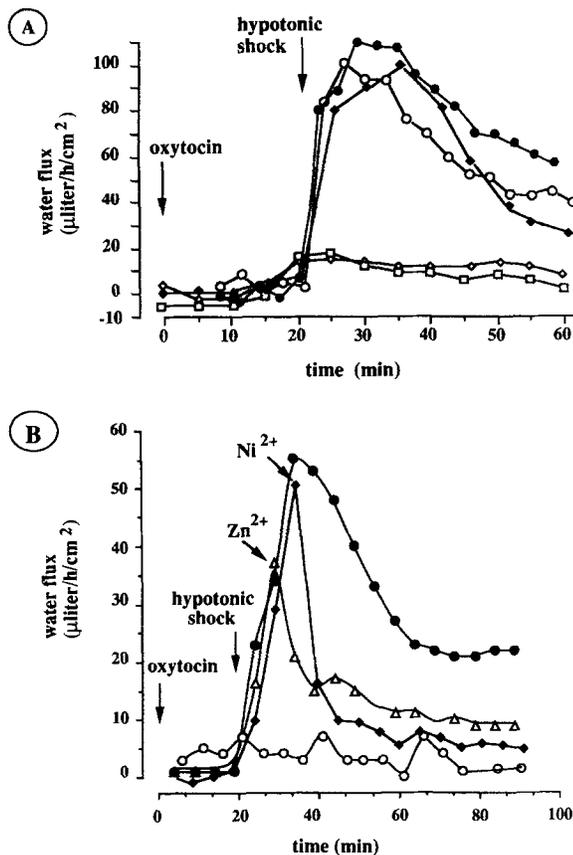
FIGURE 10. (A) Effects of luminal cyanide (O) 10^{-4} M, n = 4; 2-deoxyglucose (●) 10^{-3} M, n = 4; and Hg^{2+} (100 μM) added to luminal (□) [n = 8] or serosal side (◇) [n = 3] on net water flux induced across frog urinary bladder sacs after treatment with oxytocin (50 mU/ml in serosal solution) and hypotonic shock (half-strength Ringers solution on apical side). Control bladders (◆) [n = 19]. (B) Effects of serosal Zn^{2+} or Ni^{2+} on oxytocin-induced hydroosmotic water flux. Zn^{2+} (100 μM) was added simultaneously with the onset of the osmotic gradient (O) [n = 8] or during the rising phase of net water flux (△) [n = 3] and Ni^{2+} (100 μM) at the time of peak water flow (◆) [n = 3]. Control bladders (●) [n = 10].

followed by a hypotonic shock was used in an attempt to confine the effects of inhibitors to post cAMP steps controlling water flux. Cellular metabolism was shown not to be involved in the water response using the hypotonic shock method since J_{H_2O} was not significantly affected by cyanide (10^{-4} M) or 2-deoxyglucose (10^{-4} M) (Fig. 10 A).

The oxytocin-induced hydroosmotic water flow was very sensitive to micromolar concentrations of the heavy metals. Hg^{2+} (100 μM) added to either luminal or serosal solutions at the same time as the hypotonic shock completely prevented J_{H_2O} (Fig.

10 *A*). Serosal addition of Zn^{2+} or Ni^{2+} (100 μM) also produced complete block of J_{H_2O} when present simultaneously with the osmotic gradient (Fig. 10 *B*). Zn^{2+} or Ni^{2+} caused an immediate reduction in J_{H_2O} when added to the serosal solution of activated bladders (Fig. 10 *B*). The concentration of Zn^{2+} required to reduce the peak J_{H_2O} by 50% was 24 ± 5 μmol/liter (*n* = 5).

Block of Water Flux by Inhibitors of H⁺-ATPase

Dicyclohexylcarbodiimide (DCCD) and oligomycin have been used successfully to block proton conductance in the mitochondrial F_0 proton channel (Sebald et al., 1982). DCCD (10^{-4} M) added to the luminal solution at the same time as the osmotic shock decreased J_{H_2O} by 75% when compared to activated hemibladder controls (Fig. 11). Serosal addition of DCCD had no effect on J_{H_2O}. Oligomycin (10^{-8} M) completely prevented water flux when present at the apical side at the onset of the osmotic gradient (Fig. 11). DES blocks H⁺ ATPase in acidifying epithelia such as renal
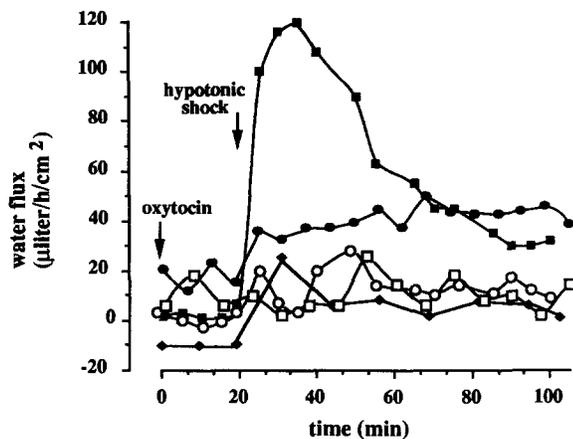
FIGURE 11. Effects on oxytocin-induced hydroosmotic water flux of proton ATPase inhibitors. DCCD (O) 10^{-5} M, *n* = 8; oligomycin (◆) 10^{-8} M, *n* = 8; NEM (●) 10^{-4} M, *n* = 4; and diethylstilbestrol (□) 10^{-5} M, *n* = 8. The inhibitors were added to luminal solution of frog urinary bladder sacs at the onset of the hypotonic shock. Control bladders (■) *n* = 8.

collecting tubule (Sabolic and Burckhardt, 1986, 1988) and frog skin (Ehrenfeld et al., 1990) and prevented J_{H_2O} when added at 10^{-5} M to the luminal side at the moment of the osmotic shock (Fig. 11). NEM, an inhibitor of vacuolar-type H⁺-ATPase and plasma membrane H⁺-ATPase in renal tubule and frog skin (Forgac, 1989; Stone and Xie, 1989; Sabolic and Burckhardt, 1986; Ehrenfeld et al., 1990; Sabatini et al., 1990) blocked ADH-induced water flux by 85% when present at 10^{-4} M in the luminal solution at the onset of osmotic shock (Fig. 11).

Site of Action of H⁺-ATPase Inhibitors

In view of the known nonspecificity of the inhibitors of proton translocating ATPases we attempted to localize the site of action on J_{H_2O} of some of these agents. Our method of inducing J_{H_2O} ought to confine inhibition to a post-cAMP step, either at the level of the water channel or interference with the normal shuttling of water channels to the plasma membrane. From the cyanide and 2-deoxyglucose experiments we have

already established that mitochondrial respiration is not involved. ADH-induced water flux requires an intact cytoskeleton (Taylor et al., 1973; Pearl and Taylor, 1983; Hardy, 1985) and it is possible that inhibition of J_{H_2O} could have arisen from interference with the transport and fusion of aggrephores to the apical cell membranes. To distinguish between these possibilities we attempted to stabilize the water channels in the plasma membrane. When ADH-treated urinary bladders are briefly exposed to a weak solution of glutaraldehyde (0.1%), water flux becomes insensitive to inhibitors of cytoskeletal function, and the water permeation pathway is fixed in an open state (Eggena, 1983; Aboulafia and Lacaz-Vieira, 1985). This technique should allow distinction between a direct inhibition of J_{H_2O} at the level of the water channel and indirect effects via the cytoskeleton.
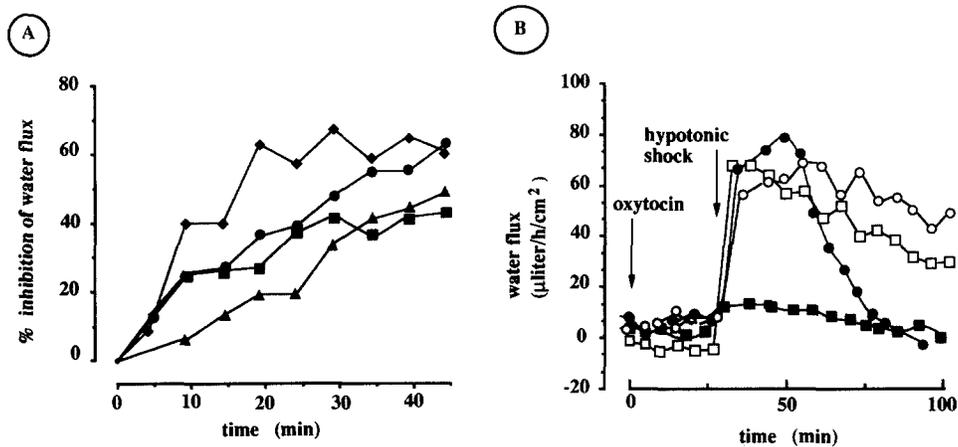
FIGURE 12.   (A) Effects of luminal addition of mercury and proton ATPase inhibitors on water flux in bladders exposed to glutaraldehyde (0.1%) for 30 s immediately before a hypotonic shock. Hg^{2+} (◆) 100 μM, $n = 5$; oligomycin (●) 10^{-6} M, $n = 4$; DCCD (■) 10^{-5} M, $n = 5$; and DES (▲) 10^{-5} M, $n = 2$. Ordinate: inhibition expressed as percentage block of the mean maximal oxytocin-activated hydroosmotic water flux measured in paired glutaraldehyde-treated bladders. Abscissa: time after addition of inhibitor to luminal solution. (B) Effects of vanadate (10^{-5} M), added to the serosal solution at the moment of osmotic shock, on oxytocin-induced hydroosmotic water flux in normal urinary bladder sacs (■) $n = 6$; and in bladders fixed in 0.1% glutaraldehyde (□) $n = 2$. Control normal bladders (●) $n = 6$; and control glutaraldehyde-fixed bladders (○) $n = 6$.

After 15 min of incubation with oxytocin, bladders were exposed to serosal half-strength Ringer containing 0.1% glutaraldehyde for 30 s, under transepithelial isotonic conditions. When this solution was replaced by control Ringer, the hyrdroosmotic water flux stabilized at high rates for long periods (>60 min) (Fig. 12 B), which is consistent with the notion that the water channels are locked in an open state. Under these conditions, oligomycin (10^{-6} M), DCCD (10^{-5} M), or DES (10^{-5} M) added to the apical solution produced significant inhibition of J_{H_2O} (Fig. 12 A). Oligomycin was the most potent inhibitor and was comparable to Hg^{2+} in its effectiveness to block J_{H_2O} (Fig. 12 A). The maximum reduction in J_{H_2O} produced by

these agents was for DCCD 43 ± 9%, n = 5; DES 49 ± 7%, n = 2; oligomycin 63 ± 8%, n = 4; and Hg^{2+} 62 ± 8%, n =5. From these data, we conclude that inhibitors of F_o-F_1 type H^+-ATPases can block water flux by a direct interaction with the water channel.

Other agents such as vanadate, have been shown to block active acid secretion via H^+ ATPase in frog skin (Ehrenfeld et al., 1985), although mitochondrial type F_1-F_o
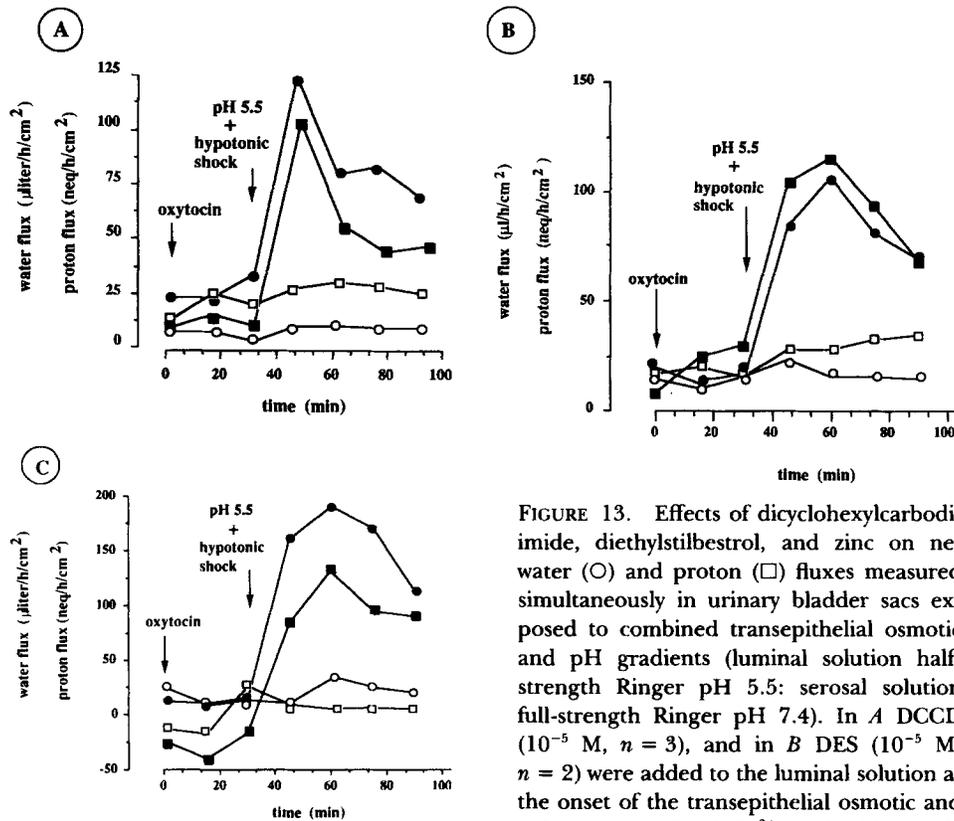
FIGURE 13. Effects of dicyclohexylcarbodiimide, diethylstilbestrol, and zinc on net water (O) and proton (□) fluxes measured simultaneously in urinary bladder sacs exposed to combined transepithelial osmotic and pH gradients (luminal solution half-strength Ringer pH 5.5: serosal solution full-strength Ringer pH 7.4). In A DCCD (10^{-5} M, n = 3), and in B DES (10^{-5} M, n = 2) were added to the luminal solution at the onset of the transepithelial osmotic and pH gradients. In C Zn^{2+} (100 µM, n = 3) was added to the serosal solution simultaneously with the transepithelial osmotic and pH gradients. Control response of water flow (●) and proton flux (■) are given for matched oxytocin-activated bladders.

H^+-ATPase is considered to be resistant to vanadate. We found that serosal vanadate (10^{-5} M) inhibits water flux at a post-cAMP step (Fig. 12 B) in agreement with previous studies (De Sousa and Grosso, 1981; Beauwens et al., 1981). The effects of vanadate on transepithelial transport of H^+ and water is thought to be nonselective (Fanestil, 1980) and the loss of its blocking power on water flux in glutaraldehyde-fixed bladders (Fig. 12 B) points to an indirect effect of vanadate on cytoskeletal events controlling insertion of water channels into the plasma membrane.

Comparison of Oxytocin-induced Titratable H^+ Flux and Water Flow

The activation and inhibition characteristics of the ADH-induced H^+ and H_2O transport were compared by simultaneously measuring J_{H_2O} and transepithelial titratable H^+ fluxes in urinary bladders exposed to a combined transepithelial pH gradient (luminal pH 5.5, serosal pH 7.4) and an osmotic gradient (half-strength Ringer apical side, normal Ringer serosal side). Oxytocin stimulated an apical to serosa directed H^+ net flux which displayed the same response pattern as the hormone activated water flux. Both the hormone induced J_{H^+} and J_{H_2O} were prevented by luminal DCCD (10^{-5} M) (Fig. 13 A) or diethylstilbestrol (10^{-5} M) (Fig. 13 B). ADH-activated J_{H_2O} and J_{H^+} were also simultaneously blocked by serosal Zn^{2+} (100 µM) (Fig. 13 C). Net water and proton fluxes were highly correlated in hormone-activated bladders (Fig. 14).
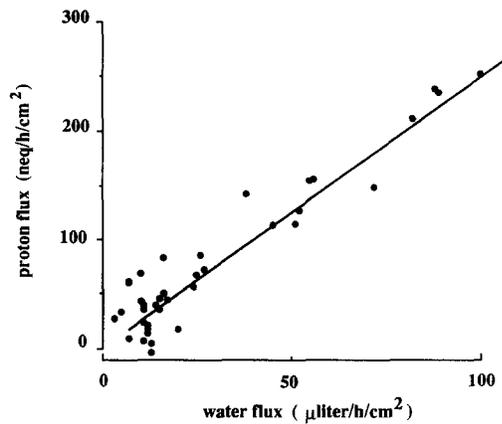
FIGURE 14. Correlation (r = 0.98) between oxytocin-activated net water flux (J_{H_2O}) and titratable H^+ flux (J_{H^+}) measured simultaneously across urinary bladder sacs exposed to combined transepithelial osmotic and pH gradients (apical solution, half-strength Ringer pH 5.5, serosal solution, normal Ringer pH 7.4).

DISCUSSION

Water and Proton Passage through ADH-induced Channels in the Apical Membrane

Current evidence indicates that ADH increases water permeability of distal urinary epithelia by inserting particle aggregates into the apical cell membranes via a cAMP-dependent mechanism (for reviews, see De Sousa and Grosso, 1981; Harris and Handler, 1988; and Handler, 1988). Studies in toad urinary bladder and mammalian collecting duct support the concept that hydroosmotic water transport occurs through very narrow and selective channels that exclude small nonelectrolytes because, although the channels possess a radius of 2Å at their narrowest point where water flow may occur by single file diffusion, they exclude small ions such as Na^+ or K^+ and they conduct protons.

Definite proof that the particle aggregates are indeed water pores or channels still remains a challenge. ADH could increase water transfer by inducing aqueous filled pores or by increasing lipid fluidity. We measured proton conductance to distinguish between these two possibilities. Because protons cross lipid bilayers with extreme difficulty but can easily jump from one molecule of water to another, ADH should

increase proton conductance if it induces aqueous filled pores, whereas if it works by increasing lipid fluidity little change should occur. In a narrow 2Å diameter channel which would constrain water flow to single file diffusion, protons can still jump from one water molecule to the next by a Grotthus chain mechanism (Glasstone and Lewis, 1960). The rapid movement of protons between hydronium ions and neighboring water molecules can explain the high conductance of H^+ in water. This transfer of protons in aqueous solutions is superimposed on the normal motion of H^+ in the electric field and permits a H^+ mobility at 25°C of 36×10^{-4} cm/s (Glasstone and Lewis, 1960). This value is close to the H^+ permeabilities that we calculated for apical and basolateral cell membranes and supports the notion that H^+ passes across these membranes through water-filled channels.

Our finding that oxytocin stimulates proton permeability at the apical cell membranes in frog skin and urinary bladder is in agreement with the demonstration by Gluck and Al-Awqati (1980) of vasopressin-induced proton conductance in urinary bladder. The H^+ flux produced by oxytocin treatment is rheogenic, producing a transepithelial current and an increase in apical membrane conductance (when the spontaneous Na^+ transport was inhibited by amiloride). In addition, we have shown that ADH exerts simultaneous effects on water and H^+ flow across the apical membranes of the principal cells. Both J_{H^+} and J_{H_2O} share similar activation and inhibition characteristics which indicate that H^+ and H_2O pass through a common channel. Oxytocin also produced changes in intracellular pH. When the electrochemical driving force for H^+ across the apical membrane favored passive H^+ influx (usually observed at external pH $\leq$ 7.4, $pH_i \geq$ 7.2 and $V_a \leq$ −25 mV) an intracellular acidification always accompanied the peak ADH response. These results agree with previous reports of an ADH induced fall in pH_i concurrent with the peak water response in toad bladder (Brem et al., 1986) and vasopressin acidification of frog skin cells (Civan et al., 1988).

Is the ADH-induced Water Channel Similar to an F_o Proton Channel?

We have shown that ADH-stimulated water and proton flux are sensitive to a wide variety of agents that inhibit H^+-ATPase pumps. Recently, it has been speculated that the water channel may have evolved from the pore forming unit of an F_1-F_o class of H^+-ATPase (Harris and Handler, 1988). This proposal, although tenuous, stems from the observations that the F_o complex forms a membrane spanning pore which permits the passage of water and H^+ (Sebald et al., 1982). Also, the mitochondrial F_o-proton channel subunits have similar molecular masses as the 7- and 14–17-kD components of ADH-induced membrane particle aggregates (water channels) identified in toad bladder (Harris et al., 1987; Harris et al., 1988). However, evidence for structural analogy between F_o and water channel subunits is lacking. Our results raise the possibility that DCCD and oligomycin may be used as probes for water and proton translocating proteins. Sulfhydryl groups may be important sites of regulation of water and proton flow through these channels since NEM (which is a very nonspecific inhibitor), is relatively specific for sulfhydryl groups, a property also shared by Hg^{2+} and pCMBS, the classical inhibitors of water flux.

H^+-ATPase pumps (representing a "new" F_1-F_o class) have been described in acid secreting urinary epithelia (Steinmetz and Andersen, 1982; Al-Awqati et al., 1983;

Brown and Hartwig, 1987; Stone and Xie, 1988) and amphibian skin (Ehrenfeld et al., 1985). It would seem that more than one type of these new proton pumps exist, given the varied pharmacology of these ATPases, and as is the case for the mitochondrial F_1-F_0 H^+-ATPase, there is no specific inhibitor available.

The classical mitochondrial-type F_1-F_0 H^+-ATPase has been identified by its sensitivity to oligomycin and DCCD (Solioz, 1984; Forgac, 1989) and proton conductance through reconstituted F_0 channels incorporated into lipid bilayers is blocked by DCCD and oligomycin (Sebald et al., 1982). The renal tubule H^+-ATPase is sensitive to DCCD, DES, and NEM (Ait-Mohamed et al., 1986; Sabolic and Burckhardt, 1988; Stone and Xie, 1988) and the H^+-ATPase of frog skin is blocked by all these agents in addition to oligomycin (Ehrenfeld et al., 1985). The ADH-induced hydroosmotic water flux, and passive rheogenic H^+ permeation were inhibited by these blockers of H^+ ATPase. In glutaraldehyde-fixed bladders these agents were still effective against J_{H_2O}, implicating a direct interaction with the water channel.

From our electrophysiological studies, we are convinced that the ADH-activated proton permeability is localized to principal cells. Although an F_1-F_0 type H^+-ATPase is present in mitochondria-rich cells in frog skin (Harvey and Ehrenfeld, 1988b), it is highly improbable that ADH-stimulated passive H^+ flux or water transfer occurs via the F_1-F_0 H^+-ATPase of these cells since this active H^+ transport pathway is unaffected by oxytocin (Ehrenfeld et al., 1989). Morever, the microelectrode recordings were made in principal granular cells which are the recognized target cells for the hormone (Harris and Handler, 1988).

To our knowledge there are no previous reports of the effects of H^+-ATPase inhibitors on ADH-induced J_{H^+} and J_{H_2O} with which we can compare our present data. It has been proposed that both "classic" mitochondrial type F_1-F_0 H^+-ATPase and the "new" F_1-F_0 proton pumps of acidifying epithelia share a common ancestry to the primordial proton pump of anaerobic bacteria (Maloney and Wilson, 1985). The ADH water channel and the F_0 proton channel share characteristics of water and H^+ conduction and sensitivity to H^+-ATPase inhibitors. Whether they also share a common ancestor will depend on the ultimate test of sequence homology of the channel subunits

H^+ and H_2O Transport across the Basolateral Cell Membranes

Much of the research into water flow in distal urinary epithelia has focussed on permeability and morphological changes induced by ADH at the apical membrane and by comparison little is known about the nature of the water transport pathway at the basolateral cell membranes. Cell volume measurements in frog skin epithelium and renal cortical collecting tubule have revealed a very high water permeabilty of basolateral membranes (MacRobbie and Ussing, 1961; Strange and Spring, 1987). If the basolateral cell membranes contain aqueous pores then this should be revealed by a Grotthus effect which should allow a water-filled channel to move 10^8 to 10^9 protons per second (Stein, 1986).

Our results show that the basolateral membranes of principal cells possess a very high spontaneous permeability to protons which can be blocked by micromolar concentrations of the heavy metals (Ni^{2+}, Cd^{2+}, Co^{2+}, Zn^{2+}, or Hg^{2+}). Bentley (1967)

has shown that Zn^{2+} blocks vasopressin-induced water flow in toad bladder and here we found that both the transepithelial hydroosmotic water flux and titratable H^+ flux in frog bladder were blocked by micromolar concentrations of Zn^{2+} or Ni^{2+}, and that both J_{H^+} and J_{H_2O} share similar K_i for Zn^{2+}. The basolateral membrane "water and proton channel" is blocked by Hg^{2+} but differs, however, from that at the apical membrane in two main respects; it is insensitive to H^+-ATPase inhibitors and it is spontaneously active and independent of ADH. It is possible that this channel is similar to the hormone insensitive water permeability described in red blood cells and in the renal proximal tubule (Whittembury and Carpa-Medina, 1988).

The involvement of a variety of commonly found epithelial ionic channels, exchangers and cotransporters were excluded as mechanisms of proton permeation across the basolateral cell membranes. The Na^+/K^+ ATPase cannot pump protons at pH > 6 and this process is blocked at $Na^+ > 6$ mM (references in Xie and Stone, 1988). Ouabain-sensitive Na^+ flux is relatively insensitive to pH_b changes between 7.4 and 5.5 (Lacoste et al., 1989) and ouabain did not affect external acid-induced changes in pH_i. A possible H^+ ATPase at the basolateral membranes was excluded by; no effect of NEM (vacuolar H^+-ATPase) or vanadate (H^+/K^+ ATPase) or DCCD (F_1-F_o H^+-ATPase). Ethoxzolamide, which was also without effect on basolateral proton current, was used to test for carbonic anhydrase dependence. Furthermore, the lack of effect of cyanide eliminates a metabolic dependence of pH_i response to low pH_b. Finally, HCO_3^--coupled transport systems are not implicated. These results point to the presence of a spontaneously open proton permeation pathway in basolateral cell membranes.

Hydrogen ion channels appear to be a rarity in animal cells, although there is evidence for Zn^{2+}-sensitive, highly selective H^+ channels in snail neuron (Thomas, 1988). An apparently similar rheogenic H^+ permeation pathway to that described here has been reported in renal epithelia (Sabolic and Burckhardt, 1983; Biagi and Sohtell, 1986; Burckhardt and Fromter, 1987). It would be interesting to discover whether the proton channels in these tissues are sensitive to heavy metals and if they also can transport water.

Is There a Physiological Role for H^+ Channels?

Given the dilute and variable acidic/alkaline nature of external solutions normally in contact with the apical surfaces of amphibian skin and bladder (pond water and urine), it is to be expected that ADH will produce simultaneous changes in net water flux and pH_i. The change in the latter could, however, be reduced under physiological conditions by a doubling of the intracellular buffering power in CO_2/HCO_3^- media (Harvey et al., 1988). Tight-junction epithelia such as amphibian skin and urinary bladder play an important role in whole body acid/base status by actively secreting H^+ via a proton ATPase pump localized in mitochondria-rich cells (Ehrenfeld et al., 1990). Through the operation of this pump, the mucosal fluid bathing these epithelia can be acidified to pH ~ 5. The ATPase-dependent acid secretion is not stimulated by ADH and a passive ADH-stimulated backflux of H^+ through water channels in the principal cells may compromise the active proton secretion process. The importance of this threat to the maintenance of net acid secretion remains to be elucidated.

There is extensive evidence that intracellular acidification blocks ADH-induced water flow at a post cAMP step (Parisi et al., 1983; Parisi and Bourguet, 1984). Intracellular pH also controls epithelial Na^+ and K^+ conductances (Harvey et al., 1988), which can be stimulated by ADH (Macknight et al., 1980; Erlij et al., 1986) and inhibited by H^+ (Onken et al., 1990). It would be interesting to discover if the ADH mediated increase in H^+ permeability and the accompanying pH_i changes are a factor in the homocellular regulation of water, Na^+ and K^+ transport responses to the hormone.
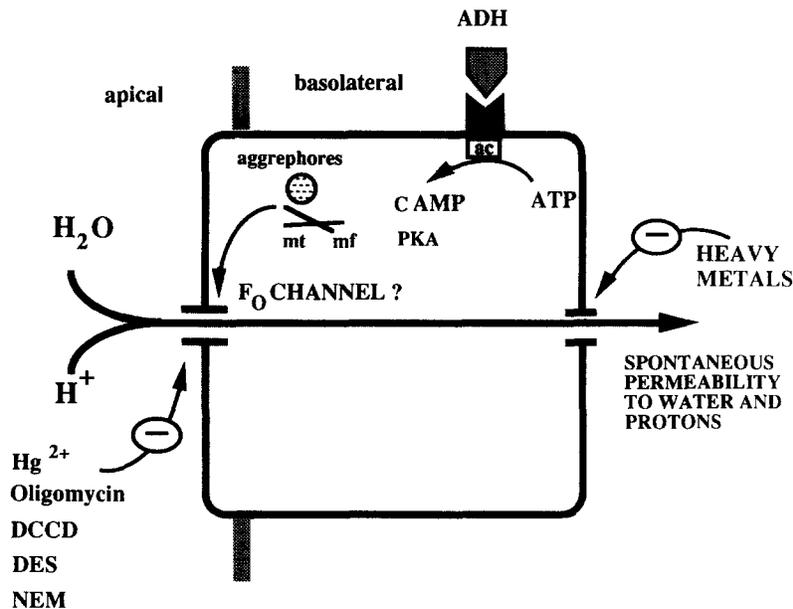
FIGURE 15. Model of the common pathways for proton and water transport across the individual cell membranes of principal cells of frog skin and urinary bladder epithelia. The basolateral cell membranes possess an aqueous-filled pore which is spontaneously open. This water channel is selective for protons and water and can be blocked by micromolar concentrations of heavy metals. The apical membrane normally has a very low permeability to water and protons which is greatly increased after treatment with antidiuretic hormone. Protons and water share a common channel at this membrane which is blocked by mercury and by inhibitors of H^+-ATPase. Since the various inhibitors shown act at a post cyclic AMP step and directly at the level of the water channel they may be used to identify and further characterize this pathway.

Conclusions

Our results are summarized in schematic form in Fig. 15. The basolateral cell membranes possess a spontaneous permeability to water and to protons which is insensitive to ADH. Both protons and water share a common spontaneously open channel at the basolateral membrane which is inhibited by the transitional heavy metals. In the absence of ADH the apical cell membranes are relatively impermeable to water and H^+. Oxytocin induces a channel with selective permeability for H^+ and

water at the apical cell membranes which is blocked by inhibitors of H^+-ATPases and by mercury. Water fluxes and rheogenic H^+ transport share a common pathway at the apical membrane. The oxytocin-induced apical water channel shares similar inhibition and permeability characteristics with an F_o-type proton channel and may have evolved from such a pore-forming protein. Although apical and basolateral membranes have highly selective water and proton permeable channels, the proteins forming these pores may be quite different. The apical proton and water permeability requires activation by ADH whereas that at the basolateral membrane is spontaneously present. Except for a similar response to mercurials, water and proton fluxes across these membranes exhibit completely different responses to transitional heavy metals and H^+-ATPase inhibitors. These properties and the proton conductivity of water channels may be exploited to gain further insights into the mechanism of water transport in ADH target tissues and in the isolation of water channels at both apical and basolateral cell membranes.

Note added in proof: A recent study by Harris et al. (1990) has shown that ADH-treated membrane vesicles from toad urinary bladder have a PCMBS-sensitive proton permeability similar to the values reported here.

REFERENCES

Aboulafia, J., and F. Lacaz-Vieira. 1985. Hydrosmotic salt effect in toad skin: urea permeability and glutaraldehyde fixation of water channels. *Journal of Membrane Biology.* 87:249–252.

Ait-Mohamed, A. K., S. Marsy, C. Barlet, G. Khadouri, and A. Doucet. 1986. Characterization of N-ethylmaleimide-sensitive proton pump in the kidney. *Journal of Biological Chemistry.* 261:12526–12533.

Al-Awqati, Q., S. Gluck, W. Reeves, and C. Cannon. 1983. Regulation of proton transport in urinary epithelia. *Journal of Experimental Biology.* 106:135–141.

Amman, D., F. Lanter, R. A. Steiner, P. Schultess, Y. Shijo, and W. Simon. 1981. Neutral carrier based hydrogen ion selective microelectrode for extracellular and intracellular studies. *Analytical Chemistry.* 53:2267–2269.

Beauwens, R., J. Crabbé, and M. Rentmeesters. 1981. Effects of vanadate on the functional properties of the isolated toad bladder. *Journal of Physiology.* 310:293–305.

Bentley, P. 1967. Mechanism of action of neurohypophyseal hormones: actions of manganese and zinc on the permeability of the toad bladder. *Journal of Endocrinology.* 39:493–506.

Biagi, B., and M. Sohtell. 1986. pH sensitivity of basolateral cell membranes of the rabbit proximal tubule. *American Journal of Physiology.* 250:F261–F266.

Brem, A. S., E. Eich, M. Pearl, and A. Taylor. 1985. Anion transport inhibitors: effects on water and sodium transport in the toad urinary bladder. *American Journal of Physiology.* 248:F594–F601.

Brem, A. S., M. Pacholski, and R. G. Lawler. 1986. Fluctuations in intracellular pH associated with vasopressin stimulation. *American Journal of Physiology.* 251:F897–F903.

Brown, D., S. Gluck, and J. Hartwig. 1987. Structure of the novel membrane-coated material in proton-secreting epithelial cells and identification as an H$^+$ ATPase. *Journal of Cell Biology.* 105:1637–1648.

Burckhardt, B. C., and E. Fromter. 1987. Evidence for OH$^-$/ H$^+$ permeation across the peritubular cell membrane of rat renal proximal tubule in HCO$_3^-$-free solutions. *Pflügers Archiv.* 409:132–137.

Carvounis, C. P., S. D. Levine, and R. M. Hays. 1979. pH dependence of water and solute transport in toad urinary bladder. *Kidney International.* 15:513–519.

Chevalier, J., J. Bourguet, and J. S. Hugon. 1970. Membrane associated particles: distribution in frog urinary bladder epithelium at rest and after oxytocin treatment. *Cell Tissue Research.* 152:129–140.

Civan, M., E. J. Cragoe, and K. Peterson-Yantorno. 1988. Intracellular pH in frog skin: effects of Na$^+$, volume and cAMP. *American Journal of Physiology.* 255:F126–F134.

De Sousa, R. C., and A. Grosso. 1981. The mode of action of vasopressin: membrane microstructure and biological transport. *Journal de Physiologie.* 77:643–669.

Eggena, P. 1983. Effect of glutaraldehyde on hydrosmotic response of toad bladder to vasopressin. *American Journal of Physiology.* 244:C37–C43.

Ehrenfeld, J., F. Garcia-Romeu, and B. J. Harvey. 1985. Electrogenic active proton pump in *Rana esculenta* skin and its role in sodium transport. *Journal of Physiology.* 359:331–355.

Ehrenfeld, J., I. Lacoste, F. Garcia-Romeu, and B. J. Harvey. 1990. Interdependence of Na$^+$ and H$^+$ transport in frog skin. *In* Animal Nutrition and Transport Processes. J. Mellinger, J. P. Truchot, and B. Lahlou, editors. S Karger, Basel, Switzerland. 6:152–170.

Ehrenfeld, J., I. Lacoste, and B. J. Harvey. 1989. The key role of the mitochondria-rich cell in Na$^+$ and H$^+$ transport across frog skin epithelium. *Pflügers Archiv.* 414:59–67.

Erlij, D., W. Van Driessche, and I. De Wolf. 1986. Oxytocin stimulates the apical K$^+$ conductance in frog skin. *Pflügers Archiv.* 407:602–606.

Fanestil, D. D. 1980. Vanadate: non-selective inhibition of transeptihelial transport of Na$^+$, H$^+$ and water. *Experientia.* 36:1045–1046.

Forgac, M. 1989. Structure and function of vacuolar class of ATP-driven proton pumps. *Physiological Reviews.* 69:765–796.

Glasstone, S., and D. Lewis. 1960. Elements of Physical Chemistry, 2nd edition. Macmillan & Co., Ltd., London. 446 pp.

Gluck, S., and Al-Awqati, Q. 1980. Vasopressin increases water permeability by inducing pores. *Nature.* 284:631–632.

Handler, J. S. 1988. Antidiuretic hormone moves membranes. *American Journal of Physiology.* 255:F375–F382.

Hardy, M. A. 1985. Microfilaments and the effects of antidiuretic hormone on water permeability. *American Journal of Physiology.* 248:C183–C184.

Harris, H. W., and J. S. Handler. 1988. The role of membrane turnover in the water permeability response to antidiuretic hormone. *Journal of Membrane Biology.* 103:207–216.

Harris, H. W., Jr., D. Kikeri, A. Janoshazi, A. K. Solomon, and M. L. Zeidel. 1990. High proton flux through membranes containing antidiuretic hormone water channels. *American Journal of Physiology.* 259:F366–F371.

Harris, H. W., H. R. Murphy, M. C. Willingham, and J. S. Handler. 1987. Isolation and characterization of specialized regions of toad urinary bladder apical plasma membrane involved in the water permeability response to antidiuretic hormone. *Journal of Membrane Biology.* 96:175–186.

Harris, H. W., Jr., J. B. Wade, and J. S. Handler. 1988. Identification of specific apical membrane polypeptides associated with an antidiuretic hormone-elicited water permeability increase in toad urinary bladder. *Proceedings of the National Academy of Sciences, USA.* 85:1942–1946.

Harvey, B. J., and J. Ehrenfeld. 1986. Regulation of intracellular pH and sodium by an electrogenic H^+ pump in frog skin. *Pflügers Archiv.* 406:362–366.

Harvey, B. J., and J. Ehrenfeld. 1988a. Role of Na^+/H^+ exchange in the control of intracellular pH and cell membrane conductances in frog skin epithelium. *Journal of General Physiology.* 92:793–810.

Harvey, B. J., and J. Ehrenfeld. 1988b. Epithelial pH and ion transport regulation by proton pumps and exchangers. *Ciba Foundation Symposium.* 139:139–164.

Harvey, B. J., and R. P. Kernan. 1984. Sodium-selective microelectrode study of apical permeability in frog skin. *Journal of Physiology.* 356:359–374.

Harvey, B. J., I. Lacoste, and J. Ehrenfeld. 1989. Common channels for water and proton passage across frog skin and urinary bladder epithelia. *Archives Internationales de Physiologie et de Biochimie.* 92:A152.

Harvey, B. J., S. R. Thomas, and J. Ehrenfeld. 1988. Intracellular pH controls cell membrane Na^+ and K^+ conductances and transport in frog skin epithelium. *Journal of General Physiology.* 92:767–791.

Ibarra, C., P. Ripoche, and J. Bourguet. 1989. Effect of mercurial compounds on net water transport and intramembrane particle aggregates in ADH-treated frog urinary bladder. *Journal of Membrane Biology.* 110:115–126.

Lacoste, I., J. Ehrenfeld, and B. J. Harvey. 1989. Sensitivity of Na/K ATPase to intracellular Ca, pH and Na in frog skin epithelium. *Archives Internationales de Physiologie et de Biochimie.* 97:C23.

Maetz, J. 1968. Salt and water metabolism. In Perspectives in Endocrinology: Hormones in the Lives of the Lower Vertebrates. E. J. W. Barrington and C. B. Jorgensen, editors. Academic Press, Inc., New York.

Macknight, A. D. C., D. R. DiBona, and A. Leaf. 1980. Sodium transport across toad urinary bladder: a model "tight" epithelium. *Physiological Reviews.* 60:615–715.

MacRobbie, E. A. C., and H. H. Ussing. 1961. Osmotic behaviour of the epithelial cells of frog skin. *Acta Physiologica Scandinavica.* 53:348–365.

Maloney, P. C. and T. A. Wilson. 1985. The evolution of ion pumps. *Bioscience.* 35:43–48.

Nelson, N. 1981. Proton ATPase of chloroplasts. *Current Topics in Bioenergetics.* 11:1–33.

Onken, H., W. Zeiske, and B. Harvey. 1990. pH-dependence and chemical modification of apical K^+ conductance in frog skin: indication of two channel populations. *Biochimica et Biophysica Acta.* 1024:95–102.

Palmer, L. G. 1982. Ion selectivity of the apical membrane Na channel in the toad urinary bladder. *Journal of Membrane Biology.* 67:91–98.

Parisi, M., and J. Bourguet. 1984. Effects of cellular acidification on ADH-induced intramembrane particle aggregates. *American Journal of Physiology.* 246:C157–C159.

Parisi, M., J. Wietzerbin, and J. Bourguet. 1983. Intracellular pH, transepithelial pH gradients and ADH induced water channels. *American Journal of Physiology.* 244:F712–F718.

Pearl, M., and A. Taylor. 1983. Actin filaments and vasopressin stimulated water flow in toad urinary bladder. *American Journal of Physiology.* 245:C28–C39.

Sabatini, S., M. E. Laski, and N. A. Kurtzman. 1990. NEM-sensitive ATPase activity in rat nephron: effect of metabolic acidosis and alkalosis. *American Journal of Physiology.* 258:F297–F304.

Sabolic, I., and G. Burckhardt. 1983. Proton paythways in rat renal brush-border and basolateral membranes. *Biochimica et Biophysica Acta.* 734:210–220.

Sabolic, I., and G. Burckhardt. 1986. Characteristics of the proton pump in rat renal cortical endocytotic vesicles. *American Journal of Physiology.* 250:F817–F826.

Sabolic, I., and G. Burckhardt. 1988. Proton ATPase in rat renal cortical endocytic vesicles. *Biochimica et Biophysica Acta.* 937:398–410.

Sebald, W., P. Friedl, H. U. Schairer, and J. Hoppe. 1982. Structure and genetics of the H^+ conducting F_o portion of the ATP synthase. *Annals of the New York Academy of Sciences.* 402:28–44.

Senior, A. E., and J. G. Wise. 1983. The proton ATPase of bacteria and mitochondria. *Journal of Membrane Biology.* 73:105–124.

Solioz, M. 1984. Dicyclohexylcarbodiimide as a probe for proton translocating enzymes. *Trends in Biochemical Sciences.* July:309–312.

Stein, W. 1986. Transport and Diffusion across Cell Membranes. Academic Press, Inc., Orlando, FL.

Steinmetz, P. R., and O. S. Andersen. 1982. Electrogenic proton transport in epithelial membranes. *Journal of Membrane Biology.* 65:155–174.

Stone, D. K., and X.-S. Xie. 1988. Proton translocating ATPases: issues in structure and function. *Kidney International.* 33:767–774.

Strange, K., and K. R. Spring. 1987. Cell membrane water permeability of rabbit collecting duct. *Journal of Membrane Biology.* 96:27–43.

Taylor, A., M. Mamelak, E. Reaven, and R. Maffle. 1973. Vasopressin: possible role of microtubules and microfilaments in hormone action. *Science.* 181:347–350.

Thomas, R. C. 1988. Proton channels in snail neurons studied with surface pH glass microelectrodes. *In* Proton Passage Across Cell Membranes. *Ciba Foundation Symposium* 139:168–183.

Van Driessche, W. 1987. Ca^{2+} channels in the apical membrane of the toad urinary bladder. *Pflügers Archiv.* 410:243–249.

Van Driessche, W., and W. Zeiske. 1985. Ca^{2+}-sensitive, spontaneously fluctuating, cation channels in the apical membrane of the adult frog skin epithelium. *Pflügers Archiv.* 405:250–259.

Whittembury, G., and P. Carpi-Medina. 1988. Renal reabsorption of water: are there pores in proximal tubule cells? *News in Physiological Sciences.* 3:61–65.